



Published in final edited form as:

*Lasers Surg Med.* 2019 January ; 51(1): 95–103. doi:10.1002/lsm.23017.

## Feature characterization of scarring and non-scarring types of alopecia by multiphoton microscopy

Jessica Lin, BSc<sup>#1</sup>, Inga Saknite, PhD<sup>#2</sup>, Manuel Valdebran, MD<sup>2</sup>, Mihaela Balu, PhD<sup>2</sup>, Griffin Lentsch, MSc<sup>2</sup>, Joshua N. Williams, BSc<sup>2</sup>, Karsten Koenig, PhD<sup>2</sup>, Bruce J. Tromberg, PhD<sup>2</sup>, and Natasha Atanaskova Mesinkovska, MD, PhD<sup>1,2</sup>

<sup>1</sup>Department of Dermatology, University of California, Irvine, California

<sup>2</sup>Laser Microbeam and Medical Program, Beckman Laser Institute

# These authors contributed equally to this work.

### Abstract

**OBJECTIVES:** Non-invasive visualization of hair follicles is important for proper diagnosis and management of alopecia; however histological assessment remains the gold standard. Laser imaging technologies have made possible noninvasive *in vivo* evaluation of skin and hair follicle. The aim of this study was to evaluate the ability of multiphoton microscopy (MPM) to non-invasively identify morphological features that can distinguish scarring from non-scarring alopecia.

**METHODS:** MPM images were obtained from areas on the scalp affected by alopecia. Investigators blinded to the diagnosis analyzed hair follicle and shaft sizes. Patients were recruited and imaged at the UC Irvine Health Medical Center and the University of California, Irvine Beckman Laser Institute. Patients with androgenetic alopecia (AGA) and alopecia areata (AA), and scarring alopecia, in particular frontal fibrosing alopecia (FFA) were recruited and imaged from July 2016 – July 2017.

**RESULTS:** We imaged 5 normal scalp subjects and 12 patients affected by non-scarring (7 subjects) and scarring (5 subjects) alopecia. In normal and non-scarring alopecia patients, MPM identified presence of sebaceous glands associated with hair follicles. MPM images of scarring alopecia were characterized by the presence of inflammatory cells surrounding hair follicles. Measurements of hair follicle diameter sizes were found to be significantly smaller in scarring alopecia patients compared to normal ( $p < 0.001$ ) and compared to non-scarring alopecia patients ( $p = 0.046$ ); non-scarring hair follicles were also significantly smaller than normal hair follicles ( $p = 0.043$ ).

**CONCLUSIONS:** This study shows that MPM imaging can non-invasively identify morphological features that distinguish scarring from non-scarring alopecia. Further studies are

---

**Corresponding author:** Natasha Atanaskova Mesinkovska, MD, PhD, Dermatology Clinical Research Center, University of California, Irvine, 843 Health Sciences Road, Hewitt Hall 1001, Irvine, CA 92697, Phone: (949) 824-1732, Fax: (949) 824-8954, nmesinko@uci.edu.

There are no conflicts of interest to disclose for this study.

needed to validate this technique and evaluate its potential to be used as an aid for guiding treatment.

### Keywords

multiphoton microscopy; laser scanning microscopy; in vivo imaging; noninvasive imaging; dermatology; alopecia

## INTRODUCTION

Hair loss is frequently underestimated in general medical practice, although it causes a significant impact in the quality of life of patients.<sup>1</sup> Patients suffering hair loss experience higher rates of anxiety and depression compared to the general public.<sup>2</sup> Traditionally, hair loss has been classified into scarring and non-scarring conditions. In non-scarring alopecia, hair follicles are preserved with potential for hair regrowth.<sup>3</sup> In scarring alopecia, the hair follicle is irreversibly destroyed due to destruction of stem cells in the bulge area of the outer root sheath, and replaced by fibrous scar tissue, leading to permanent hair loss.<sup>4</sup>

Accurate diagnosis is important for optimal treatment and management of alopecia and can be challenging due to the limitations of histologic studies and the side effects of scalp biopsies.<sup>5</sup> Diagnostic and prognostic markers are often based on clinical evaluation, assisted by dermoscopy, and a scalp biopsy, an invasive and pain-provoking procedure particularly in the pediatric population. Histology and evaluation by a dermatopathologist is currently the gold standard and most common method for diagnosing scalp conditions highly suspicious of scarring alopecia. Histopathological features of non-scarring alopecia, such as androgenetic and alopecia areata include progressive miniaturization of terminal hair follicles with a reduction in their size.<sup>3</sup>

Sebaceous glands are an integral part of the folliculosebaceous unit and are connected to the junctional zone of the hair follicle.<sup>6</sup> The location of the sebaceous glands may vary depending on physiological or pathological reasons; they are usually localized to the upper permanent part of the hair follicle in close proximity to the infundibulum.<sup>7</sup> In non-scarring alopecias, sebaceous glands are preserved and appear to be larger when compared with the miniaturized hair follicles.<sup>3</sup> Scarring alopecias, such as frontal fibrosing alopecia, are characterized histologically by lymphocytic infiltrates affecting the bulge and isthmus regions with loss of sebaceous glands. Eventually the hair follicle is replaced by a sclerotic collagenous follicular scar.<sup>8</sup>

The ability to visualize these features is critical for a correct diagnosis. Several scalp imaging techniques have been implemented in an effort to provide the dermatologists with a non-invasive tool for alopecia diagnosis.<sup>9</sup> Laser scanning microscopy is unique among optical imaging techniques in that it generates 3D, label-free, real time images with sub-micron resolution, providing access non-invasively to the morphological features used in histopathology. Reflectance confocal microscopy (RCM), a laser scanning microscopy technique with a contrast mechanism based on variations of the refractive index in the tissue, has been employed for identifying features characterizing scarring and non-scarring alopecia.<sup>10</sup>

Multiphoton microscopy (MPM) is a laser scanning microscopy technique recently translated into clinical research.<sup>11</sup> In skin imaging, MPM contrast is derived from second harmonic generation (SHG) of collagen and two-photon excited fluorescence (TPEF) of the autofluorescent species such as the co-factors NADH and FAD, elastin, keratin, and melanin. Owing to these contrast mechanisms, MPM can produce images of the cellular structure of the epidermis as well as of the elastin and collagen fibers in the extra-cellular matrix. It can also visualize cellular structures in the dermis with high contrast through the NADH fluorescence. For alopecia imaging, this is important for correctly identifying the presence of inflammatory cells in the hair vicinity in scarring alopecia.

In this pilot study, we sought to evaluate the ability of MPM to non-invasively identify morphological features that can distinguish scarring from non-scarring alopecia. We assessed qualitatively and quantitatively morphological features in MPM images acquired *in vivo* from 12 patients affected by scarring and non-scarring alopecia. For comparison purposes, we have also acquired MPM images of the normal scalp of 5 subjects.

## MATERIALS AND METHODS

### MPTflex clinical tomograph

The MPM images were obtained using a commercially available laser-scanning based clinical multiphoton tomograph (MPTflex, JenLab GmbH, Germany) which consists of a tunable 690 – 1020 nm femtosecond Ti:sapphire laser, an articulated arm with near-infrared optics attached to the tomograph to reach the anatomic area of interest, and a beam scanning module. 2 photomultiplier tube (PMT) detectors are used for parallel acquisition of TPEF and SHG signals. A customized metallic ring taped on the subject's skin attaches magnetically to the objective holder in the articulated arm, minimizing motion artifacts. An excitation wavelength of 790 nm was used in this study. The TPEF signal was detected over the range of 410 to 650 nm, whereas the SHG signal was detected over a narrow spectral bandwidth of 385 to 405 nm through emission filters placed in the TPEF and SHG detection channels. A Zeiss 40X, oil-immersion objective was used for focusing into the tissue.

### Study design

This prospective pilot study was conducted according to an approved institutional review board protocol of the University of California, Irvine (UCI-HS-2016–2954). Patients with diagnoses of hair loss conditions were recruited from the dermatology clinics, University of California, Irvine.

We imaged 4 normal scalp subjects and 12 patients affected by non-scarring (7 subjects) and scarring (5 subjects) alopecia (Table 1). Written informed consent was obtained from all patients. Images in normal patients were taken from frontal scalp. Imaging sites of alopecia patients reflect the active site locations: in androgenic alopecia (AGA), frontoparietal (crown); in alopecia areata (AA), occipital scalp; in frontal fibrosing areata (FFA), frontotemporal.

The field of view for each optical section varied from  $200 \times 200 \mu\text{m}$  to  $308 \times 308 \mu\text{m}$ . Transversal sections were taken every  $5 \mu\text{m}$  from a depth of  $0 \mu\text{m}$  (stratum corneum) to

around 200  $\mu\text{m}$  (superficial dermis). The time required for each optical section was 6 seconds. The overall investigation of the affected area required the acquisition of several image stacks at different skin sites. An average of 5 stacks was taken per case and 20 optical sections per stack. All hair loss conditions were diagnosed by board certified dermatologist (NM). Scarring alopecia cases were biopsied and assessed by a dermatopathologist.

### Image analysis

All images were processed using ImageJ.<sup>12</sup> Measurements of follicular diameter and shaft sizes were performed by two investigators (IS and MV); follicle diameter sizes were measured three times by each investigator to account for the reading error. Average follicle size was calculated for each patient using all image stacks where a follicle was present. Note that not every image stack had a follicle present. Average and standard deviation was then calculated for each group: healthy volunteers, non-scarring and scarring alopecia.

We chose to measure follicle size at the depth where the follicle was the widest. It was typically at around 80 – 130  $\mu\text{m}$  deep. We then did a linear measurement of the widest part of the follicle. However, when follicle exceeded the field of view, we measured Feret's diameter of an ellipse to assess the widest diameter of the follicle (Figure 6).

Statistical analysis was performed by Two-sample T-Test. Average hair follicle/shaft diameter values of all patients in one group were compared to those in another group. Before performing the test, it was determined whether values in each group are normally distributed by performing Lilliefors test.

## RESULTS

MPM images were analyzed qualitatively by identifying features characteristic of each type of alopecia, as well as quantitatively by measuring hair follicle diameter. These findings are summarized in Table 1.

Typical MPM images of a follicle and hair shaft from a normal scalp of a volunteer are shown in Figure 1. Keratin autofluorescence allows visualization of the hair shaft along with surrounding epidermal cells lighten up by both keratin and NADH autofluorescence. The hair follicle is outlined by collagen fibers selectively imaged by SHG signal. Sebaceous glands were associated with hair follicles in the normal frontal scalp in 3 out of 4 subjects at a deeper level than found in AGA.

### Non-scarring alopecia

We imaged 7 patients affected by non-scarring alopecia: androgenetic alopecia (AGA) and alopecia areata (AA). MPM images of non-scarring alopecia patients typically showed smaller follicle size ( $196 \pm 63 \mu\text{m}$ , Table 1), compared to normal scalp volunteers ( $294 \pm 33 \mu\text{m}$ , Table 1). The hair follicle and shaft sizes were not significantly different between AGA and AA. Prominent superficially located sebaceous glands associated with hair follicles were a hallmark present in MPM images of the scalp in all the AGA patients, while these were present in only 1 of the 4 AA patients we imaged (Table 1). Hair shafts were present in most

of the hair follicles we imaged. Inflammatory cells (lymphocytes) in the dermis were noted in the vicinity of a hair follicle in one of the alopecia areata cases.

Typical MPM images of the scalp of non-scarring alopecia patients are shown in Figure 2 and Figure 3. Figure 2 shows images of a hair follicle including two thin hair shafts entering the follicular ostia and an associated large sebaceous gland of a patient affected by AGA. Figure 3 shows representative MPM images acquired on the scalp of an AA patient. The MPM images show a miniaturized hair follicle ( $152 \pm 6 \mu\text{m}$ ) compared to hair follicles imaged in normal scalps ( $294 \pm 33 \mu\text{m}$ , Table 1), with no visible sebaceous gland associated with the hair shaft.

### Scarring alopecia

We imaged 5 patients affected with frontal fibrosing alopecia (FFA), a scarring type of alopecia. The average size of the hair follicles imaged in the FFA patients ( $127 \pm 28 \mu\text{m}$ , Table 1) was typically smaller than the value measured in the non-scarring alopecia patients ( $196 \pm 63 \mu\text{m}$ , Table 1) and in the normal scalp volunteers ( $294 \pm 33 \mu\text{m}$ , Table 1). The MPM images showed hair follicles devoid of hair shafts in 3 out of the 5 FFA patients and presence of inflammatory cells in 1 of these patients. Sebaceous glands associated with hair follicles were not present in any of the MPM images of the FFA patients.

Figure 4 shows representative MPM images acquired on the scalp of a patient affected by FFA. The MPM images show a reminiscent hair follicle small in diameter ( $114 \pm 2 \mu\text{m}$ ) with no hair shaft and no sebaceous glands present. Clusters of brightly fluorescent cells, corresponding histologically to macrophages and melanophages, are present in the dermis around the hair follicle, identified through their size (15–25  $\mu\text{m}$ ), shape and location.

The mean values of the scalp hair follicle and hair shaft diameter measured in the 3 groups of patients: normal, non-scarring (AGA and AA) and scarring alopecia (FFA) are summarized in Table 1 and their distribution plotted in Figure 5.

The hair follicles of normal scalps were significantly larger ( $p < 0.043$ ) compared to the values measured in each of the other two groups: non-scarring ( $p = 0.043$ ) and scarring alopecia ( $p < 0.001$ ). The hair follicles of the scarring alopecia (FFA) patients were significantly smaller ( $p = 0.046$ ) than of the ones the non-scarring (AGA+AA) alopecia patients. However, within the non-scarring alopecia group, although hair follicles of the AGA patients were larger than those of the AA patients, the difference was not statistically significant.

The hair shafts of normal scalps were significantly larger ( $p < 0.014$ ) than values measured in each of the other two groups: non-scarring ( $p = 0.014$ ) and scarring alopecia ( $p = 0.011$ ). However, non-scarring (AGA+AA) and scarring (FFA) alopecia groups were not distinguishable based on the hair shaft diameter measurements.

## DISCUSSION

In this pilot study, we assessed the ability of MPM to image alopecia non-invasively and to potentially distinguish between scarring and non-scarring alopecia types, critical for an effective diagnosis and management of these conditions. Features that were used to characterize scarring and non-scarring alopecia were the presence of the hair follicles, size of the hair follicles and shafts, and sebaceous gland status; among these, the size of the hair follicles was found to be statistically different between scarring and non-scarring groups.

The mean value of the follicle size corresponding to the scarring alopecia group was significantly lower than the value for non-scarring alopecia patients ( $p=0.046$ ). Generally, alopecia patients had hair follicles significantly smaller than patients with normal scalp ( $p<0.043$ ). The sizes of the hair follicles we measured are comparable with previously reported histologic measurements.<sup>13</sup> MPM images showed empty hair follicles in active sites of scarring alopecia. Hair shafts were present in the follicles corresponding to normal scalp group as well as for all the non-scarring alopecia patients; however, in hair follicles affected by non-scarring alopecia the hair shafts were often miniaturized or failed to extend beyond the scalp surface, explaining the clinical manifestations of hair loss. The presence of any hair shaft growth including those below the surface level distinguishes the non-scarring versus scarring hair follicles.

Interestingly in alopecia areata, subtype universalis, we found hair follicles completely devoid of hairs only occasionally, although follicles lacking hair shafts are common histologic features for this skin condition.<sup>14</sup> The hair shafts corresponding to the non-scarring and scarring alopecia groups were similar in size, but were miniaturized compared to those of normal scalp subjects. These results do not corroborate with data reported in a study based on RCM imaging of alopecia, where shaft miniaturization was found to be insignificant in non-scarring alopecia, but represented a strong diagnosis criterion for scarring alopecia.<sup>10</sup> The scarring group in the RCM study had a different composition and composed of lupus erythematosus (LE) and lichen planopilaris (LPP), which may explain the differences in findings.

We imaged inflammatory cells, such as lymphocytes in non-scarring alopecia cases (alopecia areata) and macrophages in one of the scarring alopecia patients (FFA) in the proximity of hair follicles, in the upper dermis. Dermal infiltration of inflammatory cells has also been observed in alopecia by RCM imaging.<sup>10</sup> However, they appear to be more clearly distinguished in MPM images, mainly due to the contrast mechanism based on the TPEF signal from NADH.

An additional morphological feature identified by MPM was sebaceous glands associated to hair follicles. They were found mainly in patients with normal scalps, and superficially located in those affected by androgenetic alopecia, a non-scarring alopecia type. Sebaceous glands were rather absent in long standing alopecia areata (non-scarring) and frontal fibrosing alopecia (scarring). Preservation of sebaceous glands are usually observed in normal scalp biopsies as well as in non-scarring alopecia cases. Loss of sebaceous glands is a histological finding observed in scarring alopecias.<sup>15</sup>

In this pilot study, we demonstrated the ability of MPM to visualize non-invasively and label-free, changes in hair follicle size, sebaceous glands and inflammatory cells in skin conditions such as alopecia. These are valuable results that can be used for future studies on expanded number of patients affected by alopecia to assess the ability of MPM to monitor and guide treatment. Besides providing information about presence of hair follicles and inflammation in skin affected by alopecia, MPM can also be instrumental in evaluating hair growth during treatment. Hair growth is currently monitored by visual assessment of hair above the skin surface, a process that can take months. However, for such studies to be performed more efficiently, current technical limitations of the clinical MPM technology need to be overcome. Current challenges of this technology are related to limited field of view, limited penetration depth and scanning speed. Imaging of the deeper dermis would allow assessing for better identification of inflammatory cells in the bulge area, a histopathological hallmark for diagnosis of scarring alopecia. Scanning rapidly large areas of the skin affected by alopecia while maintaining the sub-micron resolution would provide a better evaluation of the overall morphology and a more efficient way to evaluate the changes of hair follicles. The current technical limitations of the clinical MPM technology can be addressed and implemented in future design.<sup>18,19</sup>

## Acknowledgements

This study was supported in part by the National Institutes of Health: National Institute of Biomedical Imaging and Bioengineering, Laser Microbeam and Medical Program P41-EB015890, National Cancer Institute 1R01CA195466-01 and by the Arnold and Mabel Beckman Foundation. I.S. acknowledges the support from the Fulbright Visiting Scholar Program 2016/2017. We thank Dr. Michele van Hal for her help with patient recruitment in the initial phases of the project.

This study was approved by the UCI IRB. HS# 2016-2954

## REFERENCES

1. Williamson D, Gonzalez M, Finlay AY. The effect of hair loss on quality of life. *J Eur Acad Dermatol Venereol* 2001;15(2):137–139. [PubMed: 11495520]
2. Hordinsky M, Ericson M. Autoimmunity: alopecia areata. *J Invest Dermatol Symp Proc* 2004;9(1):73–78.
3. Bernardez C, Molina-Ruiz AM, Requena L. Histologic features of alopecias-part I: nonscarring alopecias. *Actas Dermosifiliogr* 2015;106(3):158–167. [PubMed: 25444580]
4. Filbrandt R, Rufaut N, Jones L, Sinclair R. Primary cicatricial alopecia: diagnosis and treatment. *CMAJ* 2013;185(18):1579–1585. [PubMed: 23695609]
5. Tosti A, Torres F. Dermoscopy in the diagnosis of hair and scalp disorders. *Actas Dermosifiliogr* 2009;100 Suppl 1:114–119. [PubMed: 20096205]
6. Niemann C, Horsley V. Development and homeostasis of the sebaceous gland. *Semin Cell Dev Biol* 2012;23(8):928–936. [PubMed: 22960253]
7. Genina EA, Bashkatov AN, Sinichkin YP, et al. In vitro and in vivo study of dye diffusion into the human skin and hair follicles. *J Biomed Opt* 2002;7(3):471–477. [PubMed: 12175299]
8. Whiting DA. Cicatricial alopecia: clinico-pathological findings and treatment. *Clin Dermatol* 2001;19(2):211–225. [PubMed: 11397600]
9. Otberg N, Shapiro J, Lui H, et al. Scalp Imaging Techniques. *Laser Physics Letters* 2017;14(5):055701.
10. Ardigo M, Agozzino M, Franceschini C, et al. Reflectance confocal microscopy for scarring and non-scarring alopecia real-time assessment. *Arch Dermatol Res* 2016;308(5):309–318. [PubMed: 27225248]



11. Alex A, Weingast J, Weinigel M, et al. Three-dimensional multiphoton/optical coherence tomography for diagnostic applications in dermatology. *J Biophotonics* 2013;6(4):352–362. [PubMed: 22711418]
12. Schneider CA, Rasband WS, Eliceiri KW. NIH Image to ImageJ: 25 years of image analysis. *Nat Methods* 2012;9(7):671–675. [PubMed: 22930834]
13. Kim IH, Jo HY, Cho CG, Choi HC, Oh CH. Quantitative image analysis of hair follicles in alopecia areata. *Acta Derm Venereol* 1999;79(3):214–216. [PubMed: 10384920]
14. Whiting DA. Histopathologic features of alopecia areata: a new look. *Archives of dermatology* 2003;139(12):1555–1559. [PubMed: 14676070]
15. Mirmirani P, Willey A, Headington JT, Stenn K, McCalmont TH, Price VH. Primary cicatricial alopecia: histopathologic findings do not distinguish clinical variants. *Journal of the American Academy of Dermatology* 2005;52(4):637–643. [PubMed: 15793514]
16. Kure K, Isago T, Hirayama T. Changes in the sebaceous gland in patients with male pattern hair loss (androgenic alopecia). *J Cosmet Dermatol* 2015;14(3):178–184. [PubMed: 26147300]
17. Al-Zaid T, Vanderweil S, Zembowicz A, Lyle S. Sebaceous gland loss and inflammation in scarring alopecia: a potential role in pathogenesis. *Journal of the American Academy of Dermatology* 2011;65(3):597–603. [PubMed: 21669475]
18. Balu M, Mikami H, Hou J, Potma EO, Tromberg BJ. Rapid mesoscale multiphoton microscopy of human skin. *Biomed Opt Express* 2016;7(11):4375–4387. [PubMed: 27895980]
19. Balu M, Saytashev I, Hou J, Dantus M, Tromberg BJ. Sub-40 fs, 1060-nm Yb-fiber laser enhances penetration depth in nonlinear optical microscopy of human skin. *J Biomed Opt* 2015;20(12):120501. [PubMed: 26641198]



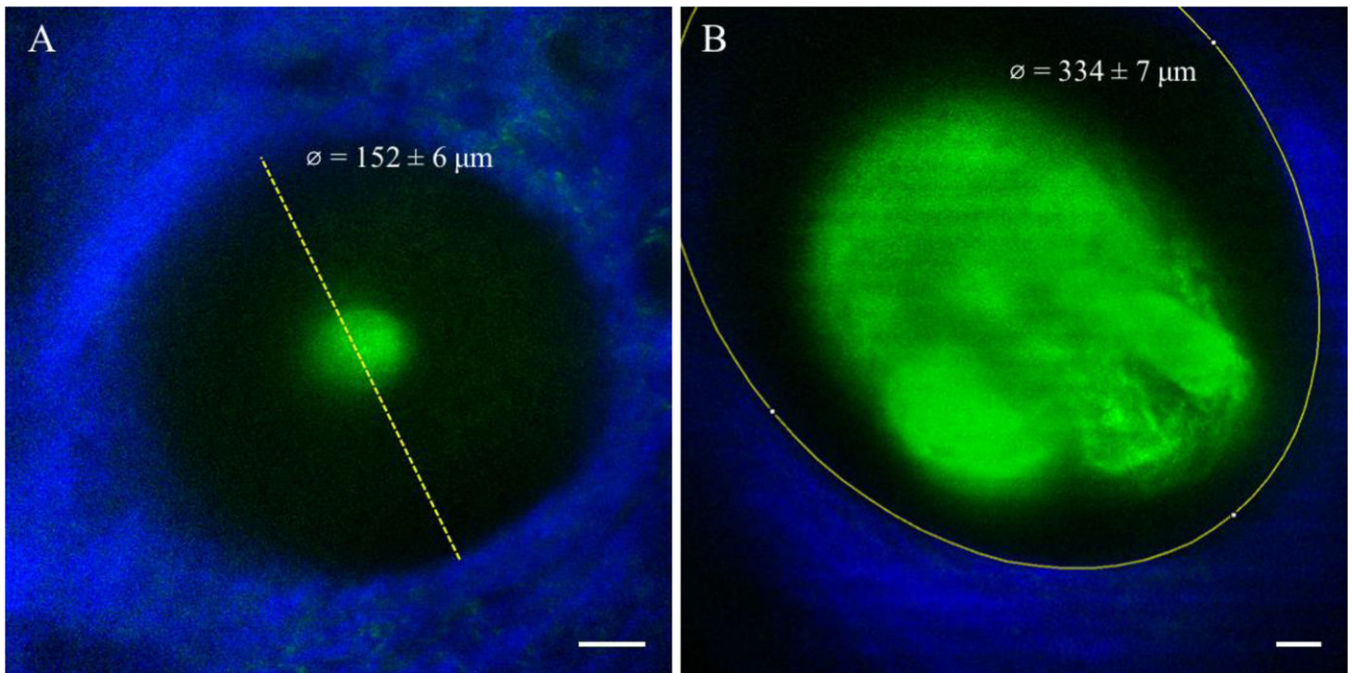


**Figure 1.**

(A) Linear measurement of the widest part of a hair follicle at a depth of 125  $\mu\text{m}$  of a non-scarring alopecia patient. Field of view is 200  $\times$  200  $\mu\text{m}$ . (B) Feret's diameter measurement of the widest part of the hair follicle at a depth of 125  $\mu\text{m}$  of a healthy volunteer. Field of view is 292  $\times$  292  $\mu\text{m}$ . Scale bar is 20  $\mu\text{m}$ .

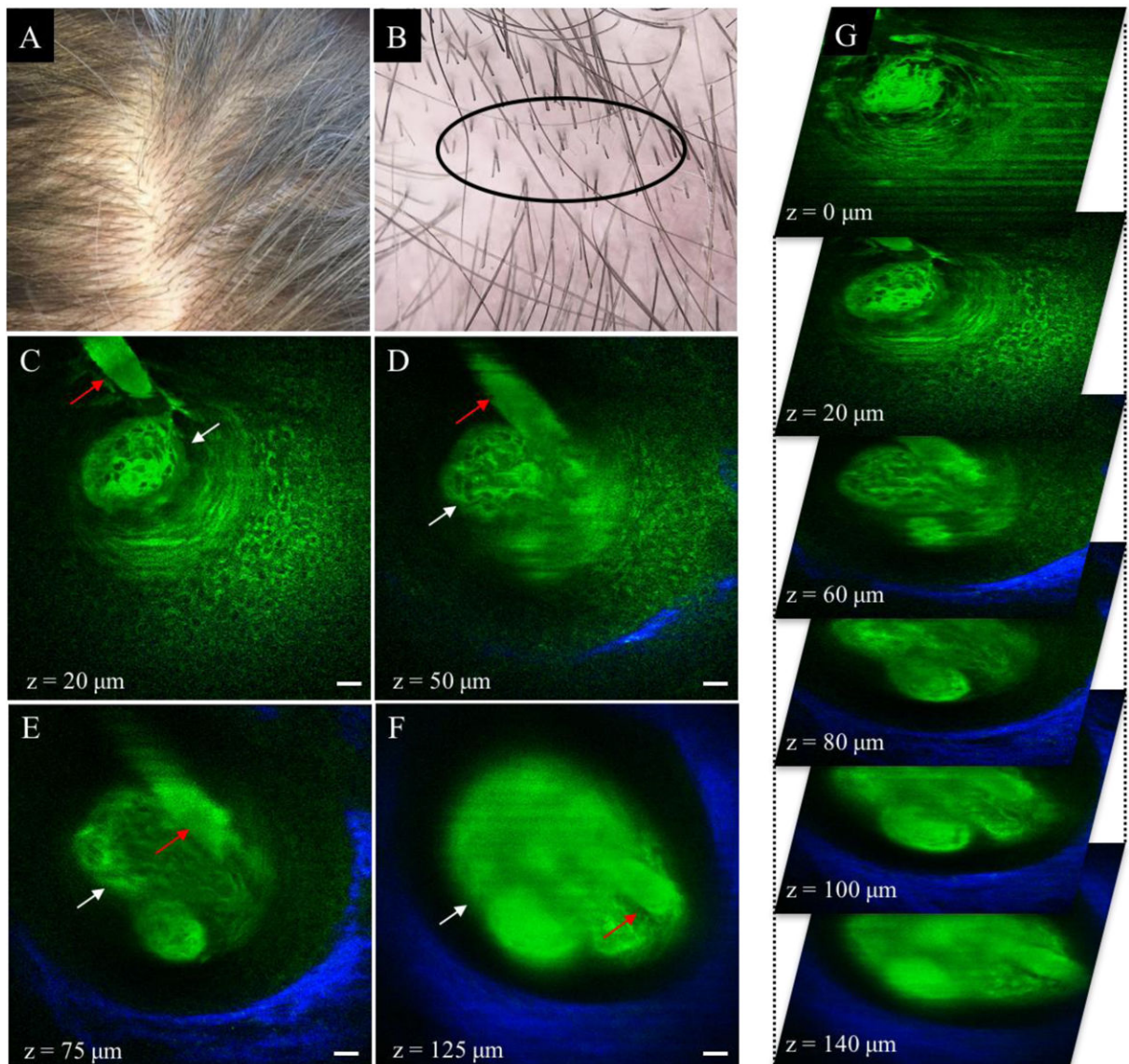


**Figure 2.**

Normal scalp (Savin I). (A) Clinical image of frontoparietal scalp area. (B) Dermoscopic image of frontoparietal scalp area. Hair was clipped in the imaged area (black ellipse). (C-F) MPM images acquired at different depths showing a hair shaft (red arrow) in the vicinity of a sebaceous gland (white arrow). The collagen fibers surrounding the hair follicle are visualized through the SHG signal (blue in D-F). Scale bar is 20  $\mu\text{m}$ . (G) A 3D view of MPM images in a z-stack from which the (C-F) images were selected.



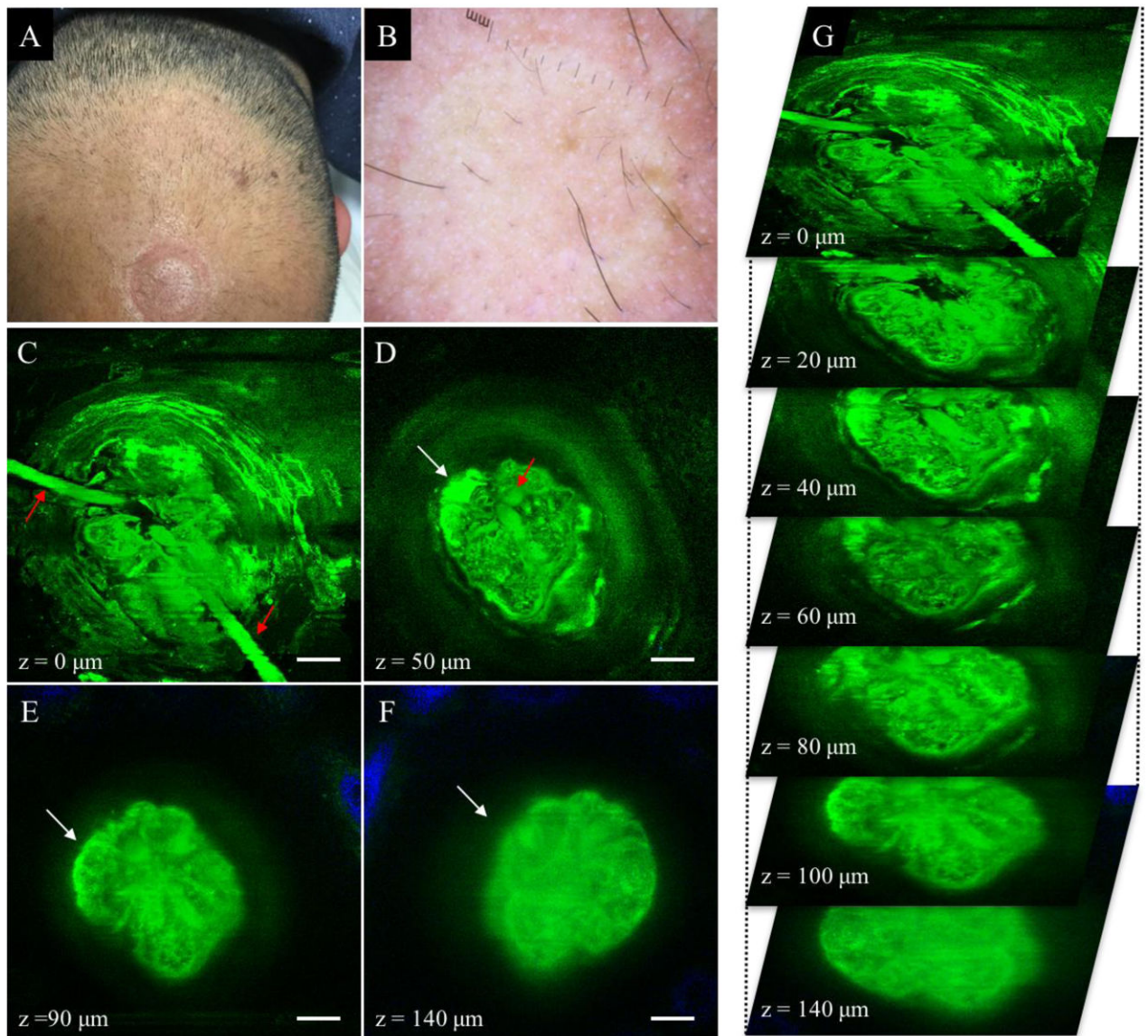


**Figure 3.** Non-scarring alopecia (AGA). (A) Clinical image of frontal scalp area affected by AGA. (B) Dermoscopic image of frontal scalp area in A. (C-F) MPM images acquired at different depths showing two hair shafts (red arrows in C-D) entering the follicular ostia and an associated superficial sebaceous gland (white arrow in D-F). Collagen surrounding the hair follicle is partly visible (blue in E and F) as it surrounds the hair follicle that is larger than the field of view. Scale bar is 20 μm. (G) A 3D view of MPM images in a z-stack from which the (C-F) images were selected.

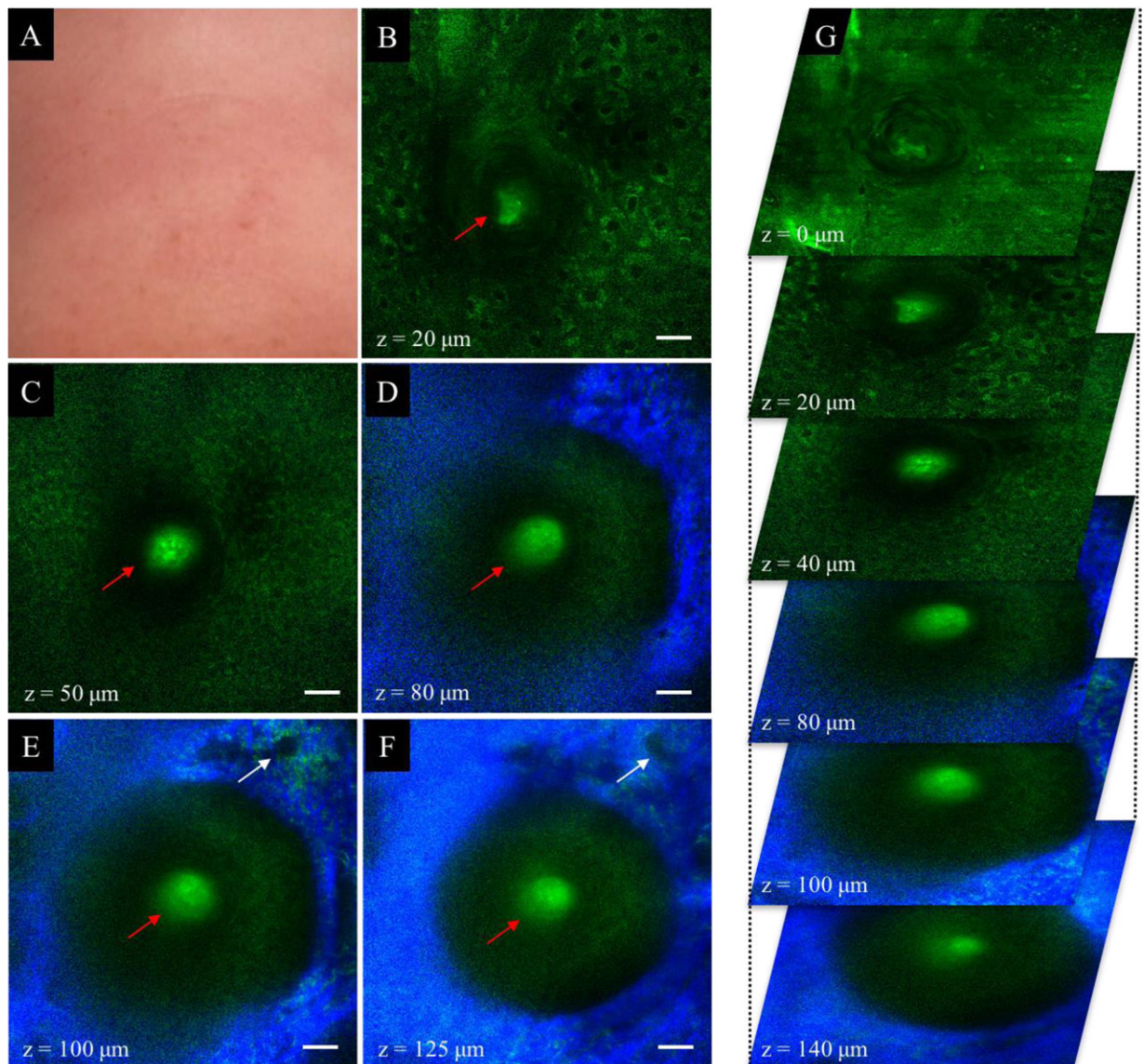


**Figure 4.**

Non-scarring alopecia (AA). (A) Clinical image of temporal scalp area affected by AA. (B-F) MPM images acquired at different depths showing a miniaturized hair follicle surrounding a hair shaft (red arrow in B-F). Epidermal cells (green) in the stratum granulosum (B) and stratum spinosum (C) surround the hair shaft and the follicular ostia. No sebaceous glands were imaged down to a depth of 125 μm. Collagen (blue) and elastin fibers (green) outline the hair follicle (D-F). A blood vessel is visible next to the hair follicle (white arrow in E-F). Scale bar is 20 μm. (G) A 3D view of MPM images in a z-stack from which the (B-F) images were selected.



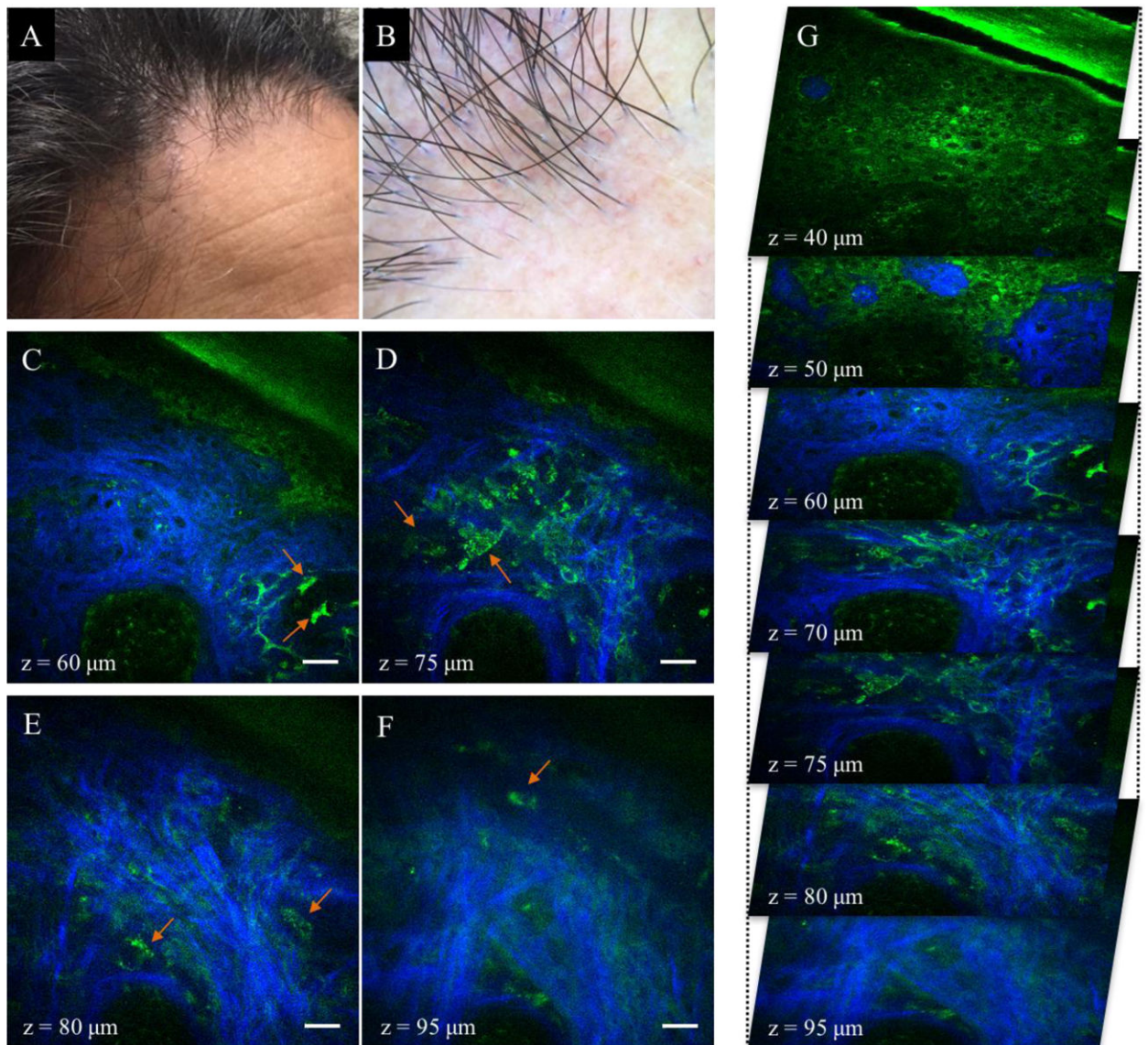


**Figure 5.** Scarring alopecia (FFA). (A) Clinical image of temporal scalp area affected by FFA. (B) Dermoscopic image of frontal scalp area in A. (C-F) MPM images acquired at different depths showing an almost obliterated empty hair follicle with no hair shaft. Sebaceous glands are notably absent. Keratinocytes are visible in the stratum granulosum and stratum spinosum layers ( $z=40\ \mu\text{m}$  and  $z=50\ \mu\text{m}$ ). Inflammatory cells (lymphocytes and macrophages, orange arrows in C-F), elastin and collagen fibers surround the follicle. Scale bar is  $20\ \mu\text{m}$ . (G) A 3D view of MPM images in a z-stack from which the (C-F) images were selected.

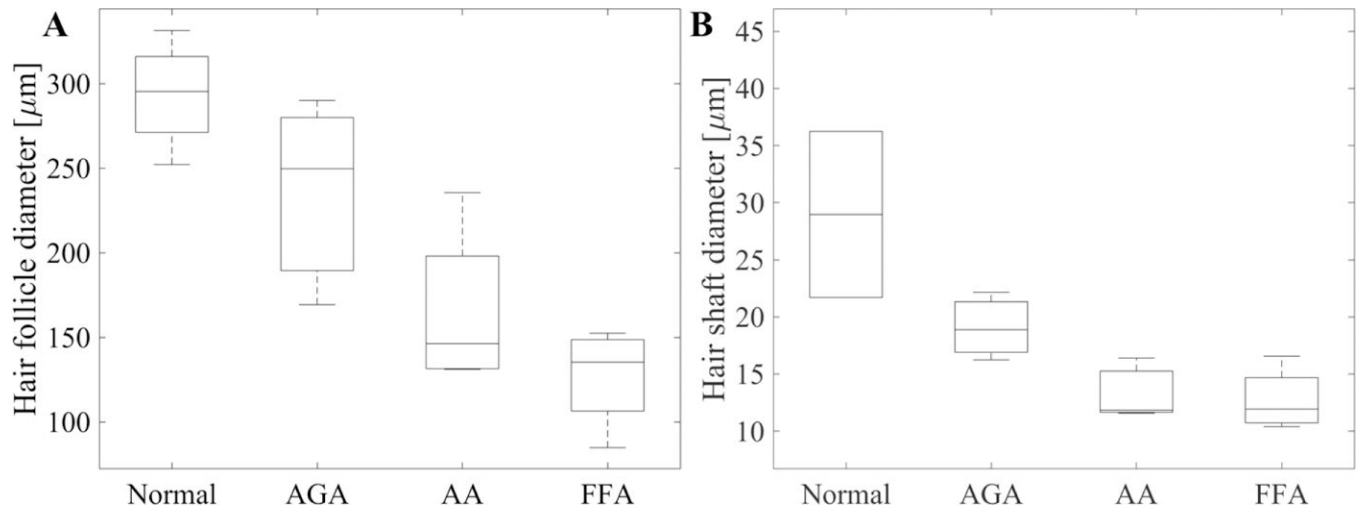


**Figure 6.** Distribution of the mean values of the hair follicle (A) and hair shaft (B) diameter corresponding to the four groups of patients: normal, androgenetic alopecia (AGA), alopecia areata (AA) and frontal fibrosing alopecia (FFA).

**Table 1.**

Summary of morphological features and hair follicle size measured in normal and alopecia scalp with MPM imaging. Values are reported as mean  $\pm$  standard deviation.

	Number of patients	Hair follicle size ( $\mu\text{m}$ )	Hair shaft size ( $\mu\text{m}$ )	Number of patients showing presence of sebaceous glands	Depth ( $\mu\text{m}$ ) at which measurements taken
Normal	4	294 $\pm$ 33	28 $\pm$ 7	3	75
Non-scarring alopecia	7	196 $\pm$ 63	16 $\pm$ 5	4	
Androgenetic alopecia	3	236 $\pm$ 61	19 $\pm$ 3	3	72
Alopecia areata	4	165 $\pm$ 49	12	1	92
Scarring alopecia (FFA)	5	127 $\pm$ 28	13 $\pm$ 3	1	68